

# Magnetic effects at the interface between non-magnetic oxides

A. BRINKMAN<sup>1\*</sup>, M. HUIJBEN<sup>1†</sup>, M. VAN ZALK<sup>1</sup>, J. HUIJBEN<sup>1</sup>, U. ZEITLER<sup>2</sup>, J. C. MAAN<sup>2</sup>, W. G. VAN DER WIEL<sup>3</sup>, G. RIJNDERS<sup>1</sup>, D. H. A. BLANK<sup>1</sup> AND H. HILGENKAMP<sup>1</sup>

<sup>1</sup>Faculty of Science and Technology and MESA+ Institute for Nanotechnology, University of Twente, 7500 AE Enschede, The Netherlands

<sup>2</sup>High Field Magnet Laboratory, Institute for Molecules and Materials, Radboud University Nijmegen, 6525 ED Nijmegen, The Netherlands

<sup>3</sup>Strategic Research Orientation NanoElectronics, MESA+ Institute for Nanotechnology, University of Twente, 7500 AE Enschede, The Netherlands

<sup>†</sup>Present address: Physics Department, University of California, Berkeley, California 94720, USA

\*e-mail: a.brinkman@utwente.nl

Published online: 3 June 2007; doi:10.1038/nmat1931

The electronic reconstruction at the interface between two insulating oxides can give rise to a highly conductive interface<sup>1,2</sup>. Here we show how, in analogy to this remarkable interface-induced conductivity, magnetism can be induced at the interface between the otherwise non-magnetic insulating perovskites SrTiO<sub>3</sub> and LaAlO<sub>3</sub>. A large negative magnetoresistance of the interface is found, together with a logarithmic temperature dependence of the sheet resistance. At low temperatures, the sheet resistance reveals magnetic hysteresis. Magnetic ordering is a key issue in solid-state science and its underlying mechanisms are still the subject of intense research. In particular, the interplay between localized magnetic moments and the spin of itinerant conduction electrons in a solid gives rise to intriguing many-body effects such as Ruderman–Kittel–Kasuya–Yosida interactions<sup>3</sup>, the Kondo effect<sup>4</sup> and carrier-induced ferromagnetism in diluted magnetic semiconductors<sup>5</sup>. The conducting oxide interface now provides a versatile system to induce and manipulate magnetic moments in otherwise non-magnetic materials.

The discovery<sup>1,2</sup> of conduction caused by electronic reconstruction at oxide interfaces has attracted a lot of interest<sup>6–13</sup>. The general structure of the perovskites ABO<sub>3</sub>, with A and B being cations, can be regarded as a stack of alternating sub-unit-cell layers of AO and BO<sub>2</sub>. A heterointerface introduces polarity discontinuities when both elements A and B on either side of the interface have different valence states. Recently, Ohtomo and Hwang<sup>2</sup> found different electronic behaviour for thin LaAlO<sub>3</sub> films on either SrO- or TiO<sub>2</sub>-terminated SrTiO<sub>3</sub> substrates, the former interface being insulating and the latter interface being an n-type conductor. Assuming the formal valence states, the polarity discontinuities can be described by either the (SrO)<sup>0</sup>–(AlO<sub>2</sub>)<sup>–</sup> or (TiO<sub>2</sub>)<sup>0</sup>–(LaO)<sup>+</sup> sequence<sup>6</sup>. Similar behaviour was found for the LaTiO<sub>3</sub>–SrTiO<sub>3</sub> interface<sup>1</sup>, resulting in a surplus of half an electron per unit cell at the TiO<sub>2</sub>–LaO interface, entering the otherwise empty conduction band. In addition to charge degrees of freedom, an induction of spin states at interfaces can also be expected. Following this scenario, a ferromagnetic alignment of the induced electron spins within the Ti-3d conduction band was theoretically predicted for the LaTiO<sub>3</sub>–SrTiO<sub>3</sub> interface<sup>14</sup> as well as for the LaAlO<sub>3</sub>–SrTiO<sub>3</sub> interface<sup>15</sup>.

To appreciate the novelty of this predicted interface magnetism, the comparison can be made to doped SrTiO<sub>3</sub>. SrTiO<sub>3</sub> is a band

insulator with a bandgap of about 3.2 eV. Doping with La<sup>3+</sup> on the Sr<sup>2+</sup> site introduces itinerant charge carriers in the conduction band. This doping gives rise to conductivity, but not to magnetism, as the Ti remains in its nominal valence 4+ state, with itinerant electrons in hybridized *spd* bands rather than localized in the 3d shell, that is, 3d<sup>0</sup>. Only when almost all Sr is replaced by La, the Ti obtains a formal valence of 3+ with a spin-1/2 local moment<sup>16</sup>, that is, 3d<sup>1</sup>. The limiting case is LaTiO<sub>3</sub>, which is an antiferromagnetic Mott insulator. The search for ferromagnetism in these systems is ongoing, but has only been successful when large amounts of magnetic elements such as several per cent of Co or at least 10% of Cr on the Ti site are added<sup>17,18</sup>. In this case, the local moments, such as the spin-3/2 Cr<sup>3+</sup> 3d<sup>3</sup> moment, give rise to magnetic effects on the transport properties when they are coupled to doping-induced itinerant charge carriers<sup>18</sup>.

To realize the SrTiO<sub>3</sub>–LaAlO<sub>3</sub> interface, we used a SrTiO<sub>3</sub>(001) substrate that was TiO<sub>2</sub>-terminated by a buffered-HF and annealing treatment<sup>19</sup>. An atomically smooth surface with clear unit-cell-height steps was observed with atomic force microscopy. On top of that, a LaAlO<sub>3</sub> film was grown at 850 °C in a wide range of partial oxygen pressures by pulsed laser deposition using a single-crystal LaAlO<sub>3</sub> target. The growth was monitored by *in situ* reflective high-energy electron diffraction<sup>20</sup>. The observed intensity oscillations clearly indicated a layer-by-layer growth mode with a very smooth surface and without any island growth. The thickness of the LaAlO<sub>3</sub> layer was 26 unit cells, approximately 10 nm, as determined from the reflective high-energy electron diffraction oscillations. After growth, the sample was slowly cooled to room temperature in oxygen at the deposition pressure. A smooth surface morphology and the correct crystal structure of the final sample were confirmed by atomic force microscopy and X-ray diffraction. X-ray photoelectron spectroscopy of a treated SrTiO<sub>3</sub> substrate and a deposited film did not show any trace of magnetic elements such as Fe, Co, Cr and Mn within a resolution of 0.1%. Four ohmic Al contacts were wire-bonded to the corners of the samples, allowing us to contact the interface and measure the transport properties without structuring the sample, which could induce damage to the interface.

The sheet resistance,  $R_s$ , as measured in a Van-der-Pauw geometry is shown in Fig. 1a for different n-type SrTiO<sub>3</sub>–LaAlO<sub>3</sub> interfaces, grown at various partial oxygen pressures (while still

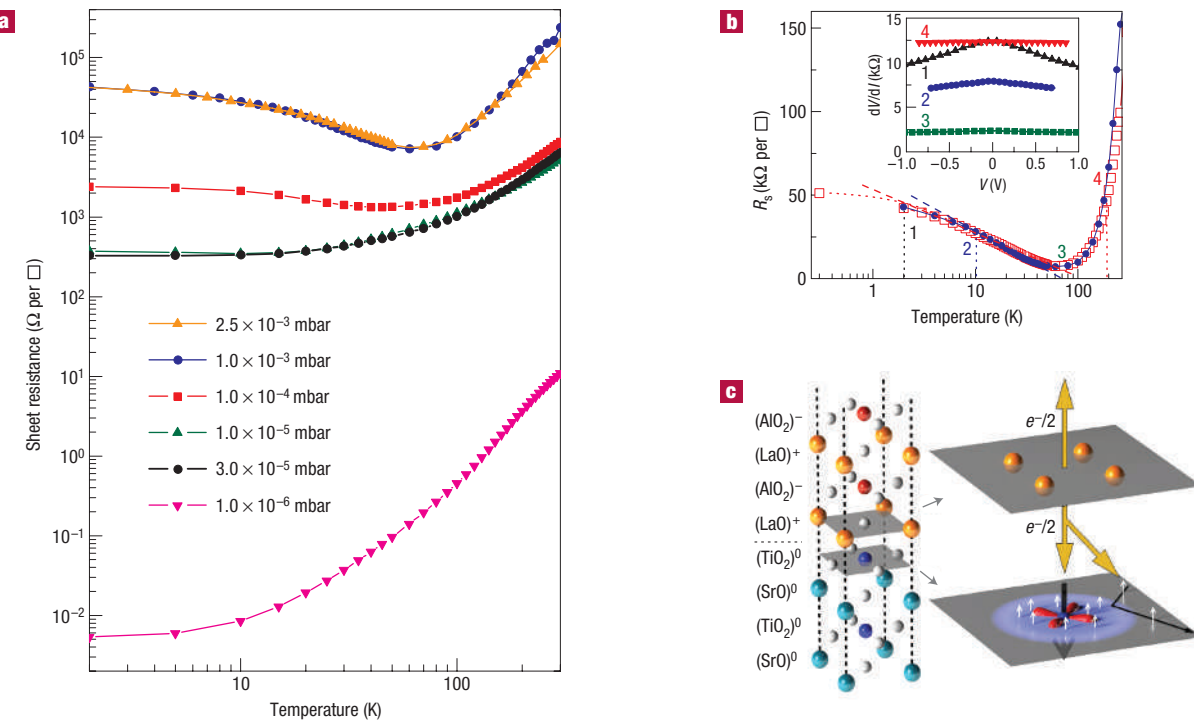


**Figure 1** Sheet resistance of n-type  $\text{SrTiO}_3$ – $\text{LaAlO}_3$  interfaces. **a**, Temperature dependence of the sheet resistance,  $R_s$ , for n-type  $\text{SrTiO}_3$ – $\text{LaAlO}_3$  conducting interfaces, grown at various partial oxygen pressures. **b**, Temperature dependence of the sheet resistance,  $R_s$ , for two conducting interfaces, grown respectively at a partial oxygen pressure of  $2.5 \times 10^{-3}$  mbar (open squares) and  $1.0 \times 10^{-3}$  mbar (filled circles). The low-temperature logarithmic dependencies are indicated by dashed lines. Inset: Four-point differential resistance  $dV/dI$  as a function of applied voltage, at a constant temperature of 2.0 K (1), 10.0 K (2), 50.0 K (3) and 180.0 K (4). **c**, Schematic representation of the electron transfer from the LaO layer into the  $\text{TiO}_2$  layer. The electrons either form localized 3d magnetic moments on the Ti site or conduction electrons that can scatter off the Kondo cloud surrounding the localized moments.

maintaining a two-dimensional growth mode), from which the presence of a conducting interface is evident. The temperature dependencies of the corresponding Hall coefficients,  $-1/eR_H$ , are shown and described as Supplementary Information. Several groups have found that oxygen vacancies give rise to conduction in oxide interfaces when the oxide layers are deposited at low oxygen pressure<sup>21,22</sup>, which also becomes clear from the dependence of  $R_s$  on the deposition conditions. From here on we will focus on the transport properties of the samples deposited at 1.0 and  $2.5 \times 10^{-3}$  mbar in which the influence of oxygen vacancies is the lowest (see the Supplementary Information).

To investigate the magnetic properties of the interface, the magnetic-field dependence of  $R_s$  is measured. Figure 2a shows the measured  $R_s$  as a function of magnetic field at different temperatures. We define the magnetoresistance as the change in resistance relative to the zero-field resistance,  $[R_s(H) - R_s(0)]/R_s(0)$ . A large negative magnetoresistance effect is observed in both samples of the order of 30% over a magnetic-field range of 30 T.

The magnetoresistance of the conducting interface is independent of the orientation of the magnetic field relative to the interface, which shows that the large magnetoresistance is related to spin physics and not to orbital effects (such as weak localization). Therefore, we assume that the observed behaviour must be ascribed to spin scattering of conduction electrons off localized magnetic moments at the interface, as we will substantiate below.

Most theoretical treatments of spin scattering in metals are elaborations of the s–d model, the non-degenerate Anderson model or the Kondo model, all of which describe the interaction between

itinerant charge carriers and localized magnetic moments<sup>23</sup>. The scattering cross-section of conduction electrons off localized magnetic moments depends on the relative spin orientation. Under an applied magnetic field, spin-flip scattering off localized moments is suppressed at the Fermi level, because of the finite Zeeman splitting between the spin-up and spin-down levels of the localized magnetic moments. The Zeeman splitting thus turns the spin scattering into an inelastic process, requiring energy exchange with the environment. The large negative magnetoresistance (up to 70%) observed in  $(\text{Sr}, \text{La})\text{TiO}_3$  alloyed with 20% of Cr has been explained by an enhanced coherent motion of the conduction electrons owing to ferromagnetically aligned spins<sup>17</sup>.

In the case of the n-type interface, the temperature dependence of the sheet resistance helps to further understand the nature of the scattering. The temperature dependence of the sheet resistance is found to be logarithmic over one decade ( $\sim 5$ – $50$  K, see Fig. 1b). The sheet resistance can be described by  $R_s = a \ln(T/T_{\text{eff}}) + bT^2 + cT^5$ , where  $T_{\text{eff}} \sim 70$  K is an effective crossover temperature scale, and where the  $T^2$  and  $T^5$  terms are suggestive of electron–electron and electron–phonon scattering, relevant at higher temperatures. Saturation of the logarithmic term is observed below  $\sim 5$  K. In addition, we observe a voltage-induced resistance suppression at low temperatures, as shown in the inset of Fig. 1b, in which a four-point differential resistance measurement is shown at the temperatures indicated in Fig. 1b.

An explanation, although still suggestive at the moment, for the observed logarithmic temperature dependence of the sheet resistance is the Kondo effect<sup>4</sup>, which describes the interplay between localized magnetic moments and mobile charge

carriers<sup>4,24,25</sup>.  $T_{\text{eff}}$  can then be interpreted as the Kondo temperature. The Kondo temperature in this definition depends on other temperature-independent scatter terms, which in the present case, however, are small, as can be seen from the depth of the minimum in Fig. 1b. The energy scale  $k_B T_{\text{eff}}$ , where  $k_B$  is the Boltzmann constant, is of the same order of magnitude as the observed energy scale  $g \mu_B H$  over which magnetoresistance effects occur, where  $g$  is the gyromagnetic factor and  $\mu_B$  is the Bohr magneton. The suppression of the Kondo effect at finite bias voltage in single-impurity (quantum dot) systems<sup>25,26</sup> arises from the fact that the Kondo resonance is pinned to the Fermi level and that an excursion of the conduction electrons from the Fermi level (owing to a finite bias) decreases the Kondo scattering. For an ensemble of impurities, it is much more difficult to apply a well-defined bias voltage, and in the present case, the voltage drop per unit cell (in our case of the order of microvolts) is only very small. Therefore, the interpretation of our experimental observations in terms of the Kondo effect is, as said, still speculative.

Magnetoresistance in spin-scattering models in general is proportional to the square of the global magnetization<sup>23</sup>,  $[R_S(H) - R_S(0)]/R_S(0) \propto -M^2(H)$ , which allows us to extract a measure of  $M(H)$  from the magnetoresistance data of Fig. 2a. The derived magnetization is shown in Fig. 2b and is linear at low magnetic fields, and saturating at high fields. The kink at small fields is an artefact of the model that does not take into account the small positive contribution to the magnetoresistance as visible in Fig. 2a. The nature of the positive contribution needs to be further investigated, but could be related to two-band conduction effects (see the Supplementary Information). The low-field susceptibility,  $\chi = dM/dH$ , for the different temperatures is plotted in the inset of Fig. 2b, from which a Curie–Weiss dependence  $\chi = C/(T + \theta)$  is found, where  $C$  is a constant and  $\theta$  is an offset temperature, characteristic for antiferromagnetic coupling at an energy scale of  $k_B\theta = 40 \mu\text{eV}$ . The competition between this energy scale and a possible Kondo singlet ground state depends on the development of the exchange interactions as a function of temperature and density of states<sup>27</sup>. A locally antiferromagnetic interaction between mobile and localized spins could in principle cause a ferromagnetic alignment of the localized spins, as in the Ruderman–Kittel–Kasuya–Yosida model of itinerant ferromagnetism<sup>3</sup>.

At 0.3 K, hysteresis appears in the sheet resistance, as shown in Fig. 3a. Again, the magnetoresistance is independent of field orientation. Magnetoresistance hysteresis is usually indicative of ferromagnetic domain formation in which domains change polarity above a certain coercive field. Domain formation typically creates a remanence in the signal when crossing zero-field, providing a butterfly shape of the magnetoresistance curve. In the present case, the shape cannot completely be explained by such an overshoot of the signal, but an additional suppression around zero-field seems to occur, which could suggest additional spin/domain reorientation effects, such as observed in granular and spin-valve giant magnetoresistance systems and the Kondo effect in quantum dots in the presence of ferromagnetism<sup>28</sup>. The presence of a small positive contribution to the magnetoresistance of Fig. 2a might be related to the shape of the hysteresis curve. We observe that the domain formation in n-type SrTiO<sub>3</sub>–LaAlO<sub>3</sub> conducting interfaces is a slow process. Figure 3b shows how the sheet resistance exponentially approaches the saturation value at a constant field of 4 T, with a time constant of about 10 s. The long time constant has also been observed in mixed-valence manganites, where phase separation between charge-ordered and ferromagnetic phases gives rise to the formation, expansion and destruction of domains<sup>29</sup>.

The explanation for the temperature dependence of  $R_S$ , the negative magnetoresistance and the observed hysteresis in n-type

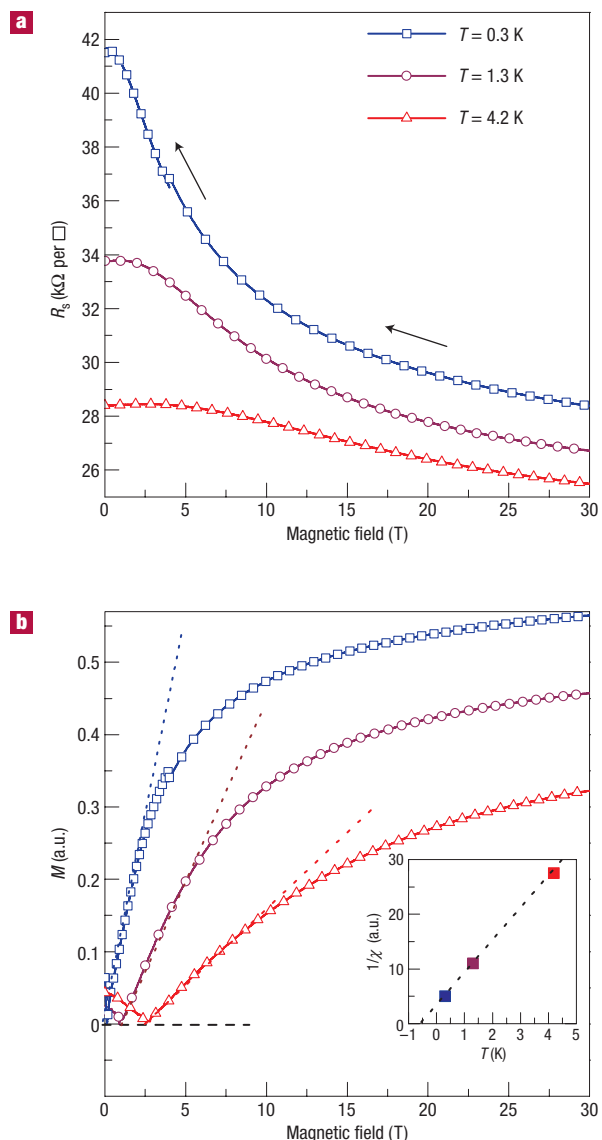


**Figure 2 Large negative magnetoresistance.** **a**, Sheet resistance,  $R_S$ , of an n-type SrTiO<sub>3</sub>–LaAlO<sub>3</sub> conducting interface, grown at  $1.0 \times 10^{-3}$  mbar, under applied magnetic field perpendicular to the interface at 0.3, 1.3 and 4.2 K. The magnetic-field sweep direction is indicated by arrows. **b**, Magnetization in units of  $g\mu_B/\pi$  as a function of the applied field, as inferred from a quadratic dependence of the magnetoresistance in **a** on magnetization. The susceptibility is derived from the linear slope at low fields. Inset: Low-field inverse susceptibility as a function of temperature, fitted by the Curie–Weiss law  $\chi = C/(T + \theta)$  with  $\theta = 0.5$  K.

SrTiO<sub>3</sub>–LaAlO<sub>3</sub> conducting interfaces in terms of the magnetic scattering centres requires the presence of magnetic moments. Magnetic effects from carrier doping or oxygen vacancies in Sr<sub>x</sub>La<sub>1-x</sub>TiO<sub>3</sub> systems have been sought for, but have never been observed<sup>17</sup>. Although very low impurity concentrations are known to give rise to the Kondo effect, for the observed strong  $R_S(T)$  minimum and large magnetoresistance of 30%, orders of magnitude more impurities (of the order of 10%, as determined from comparable experimental studies<sup>17,18</sup>) are required than the upper limit that was determined from the X-ray photoelectron spectroscopy analysis on our samples (maximally 0.1%). The necessary magnetic moments can only arise from the polar

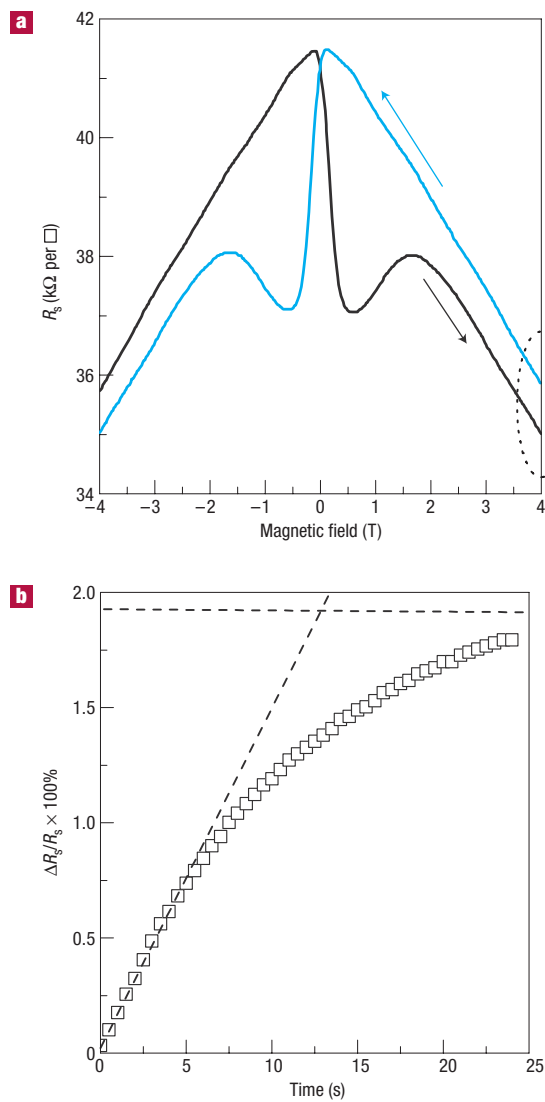


**Figure 3 Magnetic hysteresis.** **a**, Sheet resistance at 0.3 K of an n-type  $\text{SrTiO}_3\text{-LaAlO}_3$  conducting interface, grown at  $1.0 \times 10^{-3}$  mbar. The arrows indicate the direction of the measurements (at a rate of  $30 \text{ mT s}^{-1}$ ). **b**, Relative sheet resistance saturation at a constant magnetic field of 4 T, as indicated in the area enclosed by the dashed line in **a**.

discontinuity, as schematically illustrated in Fig. 1c. The interface between two non-magnetic materials has itself become magnetic.

Our present finding of a large magnetoresistance and magnetic hysteresis at the interface between  $\text{TiO}_2$ -terminated  $\text{SrTiO}_3$  and  $\text{LaAlO}_3$  also sheds light on the influence of oxygen vacancies in related interface structures. With the present observation of magnetism, we have shown that the polar discontinuity is in

fact present and that the interface conductivity cannot solely be attributed to oxygen vacancies in the considered range of deposition pressures.

The conducting oxide interface thus forms an intriguing system for studying fundamental magnetic interactions in solid-state systems and possibly opens up the way for carrier-controlled ferromagnetism in all-oxide devices.

Received 18 December 2006; accepted 2 May 2007; published 3 June 2007.

## References

- Ohtomo, A., Muller, D. A., Grazul, J. L. & Hwang, H. Y. Artificial charge-modulation in atomic-scale perovskite titanate superlattices. *Nature* **419**, 378–380 (2002).
- Ohtomo, A. & Hwang, H. Y. A high-mobility electron gas at the  $\text{LaAlO}_3/\text{SrTiO}_3$  heterointerface. *Nature* **427**, 423–426 (2004).
- Ruderman, M. A. & Kittel, C. Indirect exchange coupling of nuclear magnetic moments by conduction electrons. *Phys. Rev.* **96**, 99–102 (1954).
- Kondo, J. Resistance minimum in dilute magnetic alloys. *Prog. Theor. Phys.* **32**, 37–49 (1964).
- Dietl, T. & Ohno, H. Engineering magnetism in semiconductors. *Mater. Today* **9**, 18–26 (2006).
- Nakagawa, N., Hwang, H. Y. & Muller, D. A. Why some interfaces cannot be sharp. *Nature Mater.* **5**, 204–209 (2006).
- Okamoto, S. & Millis, A. J. Electronic reconstruction at an interface between a Mott insulator and a band insulator. *Nature* **428**, 630–633 (2004).
- Okamoto, S. & Millis, A. J. Theory of Mott insulator-band insulator heterostructures. *Phys. Rev. B* **70**, 075101 (2004).
- Hamann, D. R., Muller, D. A. & Hwang, H. Y. Lattice-polarization effects on electron-gas charge densities in ionic superlattices. *Phys. Rev. B* **73**, 195403 (2006).
- Maurice, J.-L. *et al.* Electronic conductivity and structural distortion at the interface between insulators  $\text{SrTiO}_3$  and  $\text{LaAlO}_3$ . *Phys. Status Solidi A* **203**, 2209–2214 (2006).
- Huijben, M. *et al.* Electronically coupled complementary interfaces between perovskite band insulators. *Nature Mater.* **5**, 556–560 (2006).
- Thiel, S., Hammerl, G., Schmehl, A., Schneider, C. W. & Mannhart, J. Tunable quasi-two-dimensional electron gases in oxide heterostructures. *Science* **313**, 1942–1945 (2006).
- Takizawa, M. *et al.* Photoemission from buried interfaces in  $\text{SrTiO}_3/\text{LaTiO}_3$  superlattices. *Phys. Rev. Lett.* **97**, 057601 (2006).
- Okamoto, S., Millis, A. J. & Spaldin, N. A. Lattice relaxation in oxide heterostructures:  $\text{LaTiO}_3/\text{SrTiO}_3$  superlattices. *Phys. Rev. Lett.* **97**, 056802 (2006).
- Pentcheva, R. & Pickett, W. E. Charge localization or itineracy at  $\text{LaAlO}_3/\text{SrTiO}_3$  interfaces: Hole polarons, oxygen vacancies, and mobile electrons. *Phys. Rev. B* **74**, 035112 (2006).
- Tokura, Y. *et al.* Filling dependence of electronic properties on the verge of metal-Mott-insulator transitions in  $\text{Sr}_{1-x}\text{La}_x\text{TiO}_3$ . *Phys. Rev. Lett.* **70**, 2126–2129 (1993).
- Inaba, J. & Katsufuji, T. Large magnetoresistance in spin- and carrier-doped  $\text{SrTiO}_3$ . *Phys. Rev. B* **72**, 052408 (2005).
- Herranz, G. *et al.* Co-doped  $(\text{La}, \text{Sr})\text{TiO}_{4-\delta}$ : A high Curie temperature diluted magnetic system with large spin polarization. *Phys. Rev. Lett.* **96**, 027207 (2006).
- Koster, G., Kropman, B. L., Rijnders, A. J. H. M., Blanck, D. H. A. & Rogalla, H. Quasi-ideal strontium titanate crystal surfaces through formation of Sr-hydroxide. *Appl. Phys. Lett.* **73**, 2020–2022 (1998).
- Rijnders, A. J. H. M., Koster, G., Blank, D. H. A. & Rogalla, H. In-situ monitoring during pulsed laser deposition of complex oxides using reflection high energy electron diffraction under high oxygen pressure. *Appl. Phys. Lett.* **70**, 1888–1890 (1997).
- Kalabukhov, A. S. *et al.* Effect of oxygen vacancies in the  $\text{SrTiO}_3$  substrate on the electrical properties of the  $\text{LaAlO}_3/\text{SrTiO}_3$  interface. *Phys. Rev. B* **75**, 121404 (2007).
- Siemons, W. *et al.* Origin of charge density at  $\text{LaAlO}_3$  on  $\text{SrTiO}_3$  heterointerfaces: possibility of intrinsic doping. *Phys. Rev. Lett.* **98**, 196802 (2007).
- Hewson, A. C. *The Kondo Problem to Heavy Fermions* (Cambridge Univ. Press, Cambridge, 1993).
- De Haas, W. J. & Van den Berg, G. J. The electrical resistance of gold and silver at low temperatures. *Physica* **3**, 440–449 (1936).
- Goldhaber-Gordon, D. *et al.* Kondo effect in a single-electron transistor. *Nature* **391**, 156–159 (1998).
- Van der Wiel, W. G. *et al.* The Kondo effect in the unitary limit. *Science* **289**, 2105–2108 (2000).
- Doniach, S. The Kondo lattice and weak antiferromagnetism. *Physica B+C* **91**, 231–234 (1977).
- Pasupathy, A. N. *et al.* The Kondo effect in the presence of ferromagnetism. *Science* **306**, 86–89 (2004).
- Uehara, M., Mori, S., Chen, C. H. & Cheong, S.-W. Percolative phase separation underlies colossal magnetoresistance in mixed-valence manganites. *Nature* **399**, 560–563 (1999).

## Acknowledgements

This work is part of the research program of the Foundation for Fundamental Research on Matter (FOM), financially supported by the Netherlands Organization for Scientific Research (NWO). A.B., D.B., H.H., G.R. and W.v.d.W. acknowledge additional support from NWO. The authors acknowledge J. Mannhart, A. J. Millis, R. Pentcheva and D. Winkler for useful discussions.

Correspondence and requests for materials should be addressed to A.B.

Supplementary Information accompanies this paper on [www.nature.com/naturematerials](http://www.nature.com/naturematerials).

## Competing financial interests

The authors declare no competing financial interests.

Reprints and permission information is available online at <http://npg.nature.com/reprintsandpermissions/>